ed preferentially when compared to total protein (creatine system, 120 versus 0 percent for incorporation of label; electrical stimulation system, 39 versus 29 percent for incorporation of label and 29 versus 7 percent for accumulation). The stretch model system did not preferentially stimulate accumulation of labeled amino acids into myosin, but did cause a greater accumulation of myosin compared to total protein (14.7 versus 8.7 percent, respectively). Thus, the mechanism for these changes in the stretch model system may be different from the mechanism in either the elevated creatine or electrical stimulation systems. Use of a combination of experimental model systems for studying growth regulation in skeletal muscle should help to elucidate the biochemical mechanisms involved. Once they are understood, the regulatory role of the nervous system in skeletal muscle growth may be better understood.

HERMAN VANDENBURGH
SEYMOUR KAUFMAN
Laboratory of Neurochemistry, National Institute of Mental Health, Bethesda, Maryland 20014

References and Notes

1. A. L. Goldberg, in *Cardiac Hypertrophy*, N. R. Alpert, Ed. (Academic Press, New York, 1971), p. 301.
2. J. O. Holloszy and G. W. Booth, *Annu. Rev. Physiol.* **38**, 273 (1976).
3. E. Gotschlick, *Arch. Gesamte Physiol. Menschen Tiere* **56**, 355 (1894); T. P. Feng, *J. Physiol. (London)* **74**, 441 (1932); O. Meyerhof, C. L. Gemmil, G. Benetato, *Biochem. Z.* **258**, 371 (1933); B. Katz, *Pfluegers Arch. Gesamte Physiol. Menschen Tiere* **234**, 510 (1934); U. S. von Euler, *J. Physiol. (London)* **84**, 1 (1935).
4. D. M. Stewart, in *Regulation of Organ and Tissue Growth*, R. J. Gross, Ed. (Academic Press, New York, 1972), p. 77; R. J. Tomanek, *Dev. Biol.* **42**, 305 (1975).
5. O. M. Sola and A. W. Martin, *Am. J. Physiol.* **172**, 325 (1953); T. P. Feng, H. W. Jung, W. Y. Wu, *Sheng Li Hsueh Pao* **25**, 304 (1962); D. M. Stewart, O. M. Sola, A. W. Martin, *Z. Vgl. Physiol.* **76**, 146 (1972); G. Goldspink, C. Tabary, J. C. Tabary, C. Tardieu, G. Tardieu, *J. Physiol. (London)* **236**, 733 (1974).
6. P. Thomsen and J. V. Luco, *J. Neurophysiol.* **7**, 245 (1944); S. Schiaffino and V. Hanzlikova, *Experientia* **26**, 152 (1970); E. Gutman, S. Schiaffino, V. Hanzlikova, *Exp. Neurol.* **31**, 451 (1971); E. Mackova and P. Hnik, *Physiol. Bohemoslov.* **22**, 43 (1973); S. Schiaffino, *Experientia* **30**, 1163 (1974).
7. H. H. Vandenburgh, *Biochim. Biophys. Acta* **466**, 302 (1977).
8. Cells were plated at a density of 4.25×10^3 per square millimeter (2×10^6 per frame) in 1 ml of 84 percent basal medium (Eagle's), 10 percent pretested horse serum, 5 percent chicken embryo extract, and 1 percent penicillin-streptomycin (50 unit/ml). Frames were machined from nylon (3.8 cm square by 0.65 cm high) and held together with stainless steel screws. One screw rotation equaled a 3.6 percent increase in the frame well diameter (initial diameter, 2.54 cm). An elastic silicone membrane (General Electric, MEM 213) was attached to the bottom and sides of the frame with RTV 102 cement (General Electric). The frames were washed with distilled water, coated with collagen (*7*), autoclaved, and preincubated for at least 4 hours with 1 ml of Earle's balanced salt solution in a 100-mm Falcon plastic petri dish.
9. A. L. Goldberg and H. M. Goodman, *Am. J. Physiol.* **216**, 1111 (1969).
10. A. L. Goldberg, *J. Cell Biol.* **36**, 653 (1968).
11. M. Hamosh, M. Lesch, J. Baron, S. Kaufman, *Science* **157**, 935 (1967).
12. A. L. Goldberg, *Am. J. Physiol.* **213**, 1193 (1967).
13. L. J. Elsas, F. B. Wheeler, D. J. Danner, R. L. DeHaan, *J. Biol. Chem.* **250**, 9381 (1975).
14. A. L. Goldberg, J. D. Etlinger, D. F. Goldspink, C. Jablecki, *Med. Sci. Sports* **7**, 248 (1975).
15. N. F. Clinch, *J. Physiol. (London)* **196**, 397 (1968).
16. C. K. Jablecki, J. E. Hauser, S. Kaufman, *J. Cell Biol.* **57**, 743 (1973).
17. P. Fleckman, B. R. Williams, C. E. Smith, S. Kaufman, unpublished observation.
18. C. P. Emerson and S. K. Beckner, *J. Mol. Biol.* **93**, 431 (1975).
19. J. S. Ingwall, M. F. Morales, F. E. Stockdale, *Proc. Natl. Acad. Sci. U.S.A.* **69**, 2250 (1972); J. S. Ingwall, C. D. Weiner, M. F. Morales, E. Davis, F. E. Stockdale, *J. Cell Biol.* **63**, 145 (1974).
20. A. Brevet, E. Pinto, J. Peacock, F. E. Stockdale, *Science* **193**, 1152 (1976).
21. O. H. Lowry, N. J. Rosebrough, A. L. Farr, R. J. Randall, *J. Biol. Chem.* **193**, 265 (1951).
22. B. Paterson and R. C. Strohman, *Dev. Biol.* **29**, 113 (1972).
23. I. Arndt and F. A. Pepe, *J. Histochem. Cytochem.* **23**, 159 (1975).

10 April 1978; revised 2 October 1978

Phycomyces: Modification of Spiral Growth after Mechanical Conditioning of the Cell Wall

Abstract. *Mature stage IVb* Phycomyces *sporangiophores show left-handed spiral growth; that is, viewed from above, the sporangium rotates clockwise. Mechanical conditioning of the cell wall by the Instron technique increases the ratio of the rotational to the elongational growth rate. This result is in agreement with the fibril reorientation model of spiral growth, which suggests that cell wall microfibrils, initially oriented in a nearly transverse right-handed direction in the upper region of the growing zone, are displaced during growth toward the longitudinal axis, causing the observed left-handed spiral growth.*

Although many plants show some spiral growth during development, few examples are as striking as the early developmental stages of *Phycomyces* (*1–3*). The young stage I sporangiophore shows left-handed spiral growth (clockwise rotation of the sporangium, viewed from above). In stages II and III, elongational and rotational growth cease as the sporangium enlarges and matures. After the formation of the mature sporangium spiral growth is again initiated, but this time in the right-handed direction; this stage is called IVa and lasts about 90 minutes.

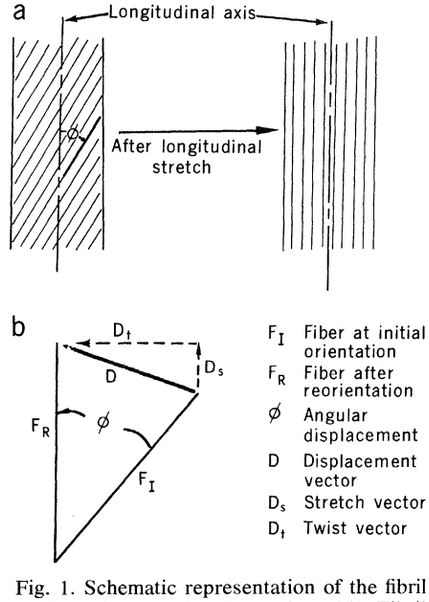

Fig. 1. Schematic representation of the fibril reorientation model [redrawn from (*4*)]. Fibril reorientation results from longitudinal stretch (a). This orientation is represented by a displacement vector **D** with components $\mathbf{D}_t$ and $\mathbf{D}_s$ (b).

During the end of this stage the rotation rate slowly decreases to zero, only to start again in the clockwise direction, which marks the last and final stage of development, called stage IVb. This entire reversal or rotation occurs during continued stalk elongation.

To our knowledge *Phycomyces* is unique in this reversal. A model to explain the mechanism of stage IVb cell wall growth has recently been proposed (*4*), based on the following two experimental findings. First, Ahlquist and Gamow (*5*) measured an abrupt change in the mechanical extensibility of the chitinous cell wall during the transition from stage II to stage IVb. During this period the cell wall changes from an essentially elastic body in stage II to a viscoelastic body in stage IVb. Second, Ortega *et al.* (*6*) found that the ratio of the rotational to the elongational growth rate was significantly larger in the lower regions of the growing zone than in the upper regions. These two experimental findings support the following model: the left-handed spiral growth of stage IVb occurs because the obliquely situated microfibrils in the primary cell wall are reorientated toward the longitudinal axis of the cell under internal turgor pressure.

Results of electron and polarizing microscopy suggest that the fibrils in the inner wall of the growing zone are either in the direction of a right-handed spiral or flatly transverse (*7–9*); in this respect the primary cell wall of *Phycomyces* is similar to the primary cell wall of most higher plants (*10*). Apparently, in the growing sporangiophore the fibrils lie in a nearly flat right-handed spiral; the measured ex-

0036-8075/79/0119-0268$00.50/0

treme configuration of the fibrils is probably a direct result both of the loss of turgor pressure and of the chemical cleaning done in preparation of the cell wall (*9*). Fibrils in the nongrowing zone lie parallel to the longitudinal axis. Figure 1 shows how the reorientation of a right-handed spiral structure could account for the observed left-handed spiral growth (*4*). The two components of spiral growth are represented as two unit vectors $\mathbf{D}_t$ and $\mathbf{D}_s$, where $\mathbf{D}_t$ is growth in the horizontal direction and $\mathbf{D}_s$ is elongational growth. The flatness of the spiral is determined by the angle ϕ. From Fig. 1 one can readily deduce that $1/\phi \cong \mathbf{D}_t/\mathbf{D}_s$ This relationship predicts that $\mathbf{D}_t/\mathbf{D}_s$ should increase with decreasing ϕ. In this report, we describe experiments done to test this prediction.

To decrease ϕ, we relied on the fact that the oblique microfibrils embedded in the viscoelastic primary cell wall are oriented toward the longitudinal axis when the cell wall is mechanically extended along its longitudinal axis. We found that after a number of such cell wall extensions the cell wall becomes mechanically elastic; that is, the amount of extension for a particular load becomes constant and this extension is totally recovered when the cell wall is unloaded (*11*). This mechanically conditioned cell wall is referred to as strain-hardened (*12*). Although we did not directly measure the decrease in ϕ after cell wall extension, the fact that the wall does become mechanically conditioned strongly suggests that the microfibrils are reoriented during mechanical extension and therefore were initially transverse in orientation. To determine the effect of ϕ on rotation and elongation, we measured the ratio of the rotational to the elongational growth rate before and after strain hardening.

Stage IVb sporangiophores were adapted to red light for at least 30 minutes; the experiments were entirely performed in red light to avoid any spurious light effects. A sporangiophore was lightly dusted with starch particles, and then an aluminum foil marker was placed on the stalk immediately below the sporangium (Fig. 2). A specially designed punch was constructed to ensure that all markers were uniform in size, and the markers were periodically measured with a calibrating (toolmaker's) microscope. The aluminum markers were rectangular, measuring 0.546 mm in length; they adhered to the cell wall by static electricity (*13*). The sporangiophore was then photographed every 2 minutes. Rotation and elongation rates can be determined from any pair of photographs. The elongation rate was determined by measuring the change in distance between the upper aluminum marker and a starch particle located somewhere below the growing zone. The rotation rate was determined by measuring the apparent change in length of the marker as it rotated about the vertical axis of the stalk. The angle of displacement of the marker from a vertical plane normal to the camera is arc cosine $L_1/L_2 = \theta$, where L_1 is the apparent length of the marker photographed in the plane normal to the camera and L_2 is the known actual length of the marker. At the start of the experiment, $L_1 = L_2$ and the arc cosine is zero. After a series of photographs were taken at 2-minute intervals, the sporangiophore was strain-hardened by using an Instron machine and the entire procedure was repeated. The average delay in growth after strain hardening was about

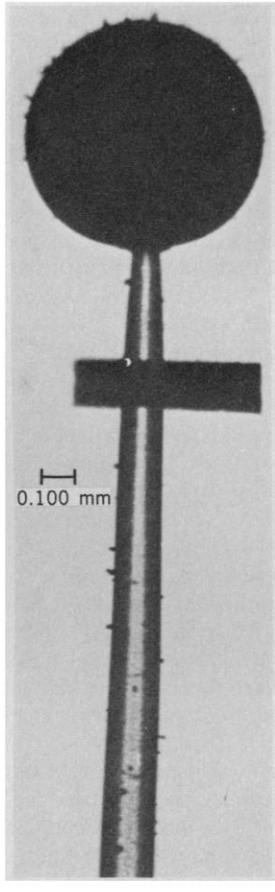

Fig. 2 (left). Stage IVb sporangiophore with an aluminum marker placed below the sporangium.

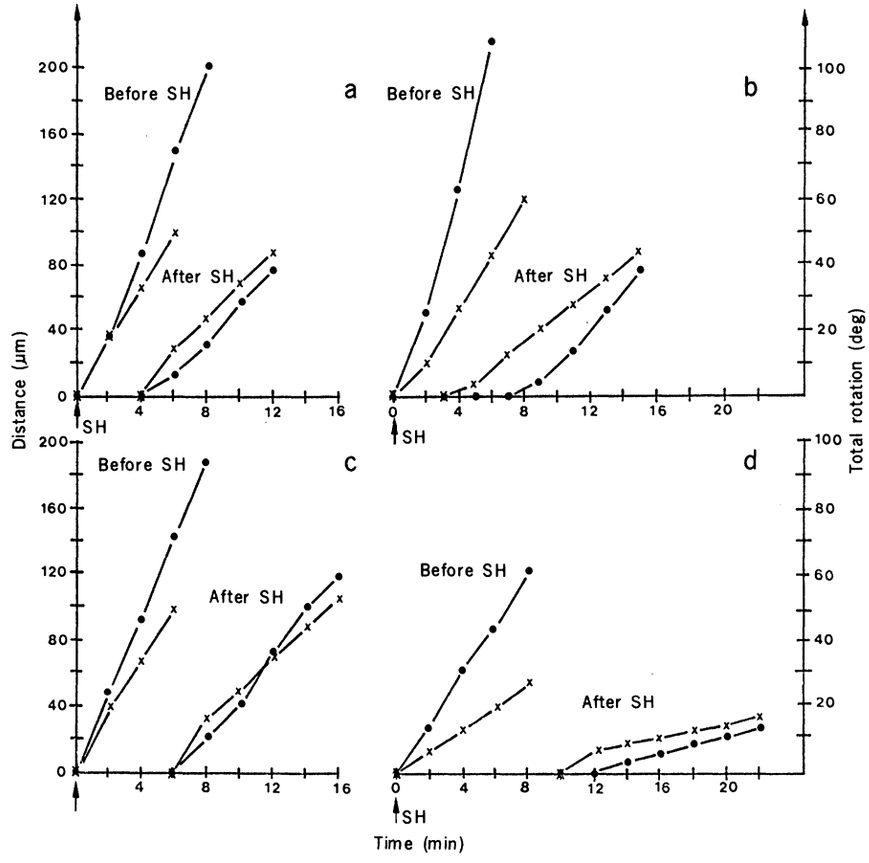

Fig. 3. Mature stage IVb sporangiophores adapted in red light were photographed every 2 minutes to determine total rotation (x) and elongation (●) rates before and after strain hardening (*SH*). Arrows indicate when strain hardening was initiated. Sporangiophores that showed neither rotation nor elongation 15 minutes after strain hardening were discarded. The data show that the rotation/elongation ratio increased after strain hardening. The data represent four identical experiments.

5 minutes. On the average, it took about 2 minutes to unhook the sporangiophore from the Instron machine and prepare it for photography.

Figure 3 shows the data from four experiments. In each case, rotation predominated over elongation, compared to the results of control experiments. We often found that right after strain hardening we could measure significant rotation rates but no elongation rate (Fig. 3, b and d). This is predicted by the fibril reorientation model (the ratio of rotation to elongation increases as ϕ decreases). As shown in Fig. 3, this relative increase in rotation stems from a disproportionate decrease in elongation after strain hardening rather than an increase in the rotation rate. The net decrease in both rotation and elongation is also consistent with the reorientation model, as shown in Fig. 1b: $\mathbf{D}_t$ and $\mathbf{D}_s$ both decrease in magnitude as ϕ decreases, but $\mathbf{D}_s$ decreases faster. Finally, we note that the increase in the ratio of the rotational to the elongational growth rate measured after strain hardening is similar to that observed in the lower region of the growing zone (*6*). It is also in agreement with the concept that the right-handed spiral configuration of microfibrils is becoming less flat in the lower region of the growing zone; that is, ϕ is progressively decreasing toward the lower region of the growing zone. In conclusion, our data are consistent with the fibril reorientation model, and to our knowledge no other proposed model predicts the change in ratios that we have measured.

R. I. GAMOW, B. BOTTGER
Department of Chemical Engineering, University of Colorado, Boulder 80309

References and Notes

1. A. J. P. Oort, *Proc. K. Ned. Akad. Wet.* **34**, 564 (1931).
2. E. S. Castle, *Am. J. Bot.* **29**, 664 (1942).
3. K. Bergman *et al.*, *Bacteriol. Rev.* **33**, 99 (1969).
4. J. K. E. Ortega and R. I. Gamow, *J. Theor. Biol.* **47**, 317 (1974).
5. C. N. Ahlquist and R. I. Gamow, *Plant Physiol.* **51**, 586 (1973).
6. J. K. E. Ortega, J. F. Harris, R. I. Gamow, *ibid.* **53**, 485 (1974).
7. A. J. P. Oort and P. A. Roelofsen, *Proc. K. Ned. Akad. Wet.* **35**, 898 (1932).
8. P. A. Roelofsen, *Biochim. Biophys. Acta* **6**, 340 (1950).
9. ——, *ibid.*, p. 357.
10. R. D. Preston, *The Physical Biology of Plant Cell Walls* (Chapman & Hall, London, 1974).
11. J. K. E. Ortega, R. I. Gamow, C. N. Ahlquist, *Plant Physiol.* **55**, 333 (1975).
12. Loading and unloading a sporangiophore alters the mechanical properties of the cell wall such that a sporangiophore having the same load a second time exhibits less extension. This change in extensibility decreases until it becomes negligible after a number of consecutive loadings. In the experiments reported here, each sporangiophore was loaded and unloaded ten times to a final load of 240 mg in less than 1/2 minute.
13. During elongational growth the markers in the upper region of the growing zone are slowly displaced away from the sporangium. These markers then can no longer be used to determine rotational and elongational rates of the entire growing zone since they reflect only cell wall changes that occur in the growing zone at or below their location.
14. Supported by NSF grants GB-31039 and GB-35597. We thank K. Foster for many fruitful discussions.

25 May 1978; revised 21 August 1978

Harmonic-Sensitive Neurons in the Auditory Cortex of the Mustache Bat

Abstract. *Human speech and animal sounds contain phonemes with prominent and meaningful harmonics. The biosonar signals of the mustache bat also contain up to four harmonics, and each consists of a long constant-frequency component followed by a short frequency-modulated component. Neurons have been found in a large cluster within auditory cortex of this bat whose responses are facilitated by combinations of two or more harmonically related tones. Moreover, the best frequencies for excitation of these neurons are closely associated with the constant-frequency components of the biosonar signals. The properties of these neurons make them well suited for identifying the signals produced by other echolocating mustache bats. They also show how meaningful components of sound are assembled by neural circuits in the central nervous system and suggest a method by which sounds with important harmonics (or formants) may be detected and recognized by the brain in other species, including humans.*

In English speech sounds, there are several types of acoustic cues or information-bearing elements (*1*). Formants—that is, constant-frequency (CF) components, are essential for recognition of vowels. Fills—noise bursts—are important for recognition of some fricative consonants. Transitions—frequency-modulated (FM) components—and voice onset time are important for recognition of plosive consonants and some fricative consonants combined with vowels. There are also FM components in other phonemes (glides). The CF, FM, and noise burst elements are found in animal sounds as well (*2*).

In response to sound, mammalian cochlear nerve fibers can send impulses into the brain in stimulus-locked (or phase-locked) fashion when the frequency or repetition rate is less than 5 kHz (*3*). Therefore it is conceivable that almost all information-bearing elements and their combinations lower than 4 kHz are processed in the form of phase-locked discharges of many auditory neurons in the brain. This may be considered an extension of the volley theory proposed for the neural basis of frequency discrimination (*4*). Several papers, however, demonstrate that auditory neurons in the cerebral cortex are commonly phasic (*5*) and show poor phase-locked discharges to sounds above 1.0 kHz (*6*), and that some of them are specialized to respond best to particular sounds (*2, 6–8*).

Therefore an alternative hypothesis (*9*) is that acoustic signals are represented by neurons arranged in coordinates of frequency and amplitude. When the amplitude spectra of the acoustic signals vary with time, the spatial pattern of the neural activity in this coordinate system would vary accordingly (*the spatiotemporal pattern theory*). In still another hypothesis, acoustic signals are eventually processed by feature detectors, and the activity of the feature detectors leads to the categorization of acoustic signals in the brain (*the detector theory*). These theories are not mutually exclusive, because the auditory system appears to use all three principles in processing acoustic signals (*6–9*). The data supporting the detector theory are, however, very limited. The major purpose of this report is to demonstrate neurons that assemble harmonically related components in animal sounds (*10*) and accordingly favor the detector theory.

To study the neural basis of acoustic pattern recognition, it is essential to know the physical properties and biological significance of the acoustic signals used by the species and to employ these signals or their information-bearing elements as stimuli, because the auditory system has evolved to detect and process biologically significant sounds. In the mustache bat, *Pteronotus parnellii rubiginosus*, the biosonar signals (also called orientation sounds or pulses) are stereotyped, moderately complex, and essential for survival. The biological significance of individual signal elements is known (*11*). Furthermore, individual information-bearing elements in ultrasonic signals cannot be coded by the volley principle. The mustache bat is thus an ideal animal in which to study neural specialization to detect particular information-bearing elements or combinations of them. In this report, we describe the response properties of harmonic-sensitive neurons in the auditory cortex of

0036-8075/79/0119-0270$01.00/0